Simultaneous Detection and Parallel Interference Cancellation in GFDM for 5G

Juan Pablo Mayoral Arteaga, Rodrigo Pereira David and Raimundo Sampaio Neto

***Abstract*— The generalized frequency division multiplexing transmission technique (GFDM), is being discussed as a candidate waveform for the fifth generation wireless communication system (5G). Since it only uses one cyclic prefix (CP) per group of symbols instead of one CP per symbol, the GFDM technique is more spectrally efficient than the traditional OFDM systems. In this work we propose a low complexity detection scheme for GFDM where a matched filter (MF) detection is used in conjunction with the parallel interference cancellation technique (PIC). In addition to reducing the complexity of the receiver, the proposed scheme incorporates a strategy to dynamically limit the number of iterations of the PIC. Performance results are presented in terms of information symbol error rate (SER).**

***Keywords*— GFDM vs OFDM, signal generation, Matched Filter detection, Parallel Interference Cancellation technique, performance, 5G.**

I. Introduction

Mobile communications networks are experiencing a substantial increase in data traffic due to the several emerging applications, such as Machine-to-Machine communications (M2M), Internet of Things (IoT), Tactile Internet [1], [2] as well as novel broadband services like ultra High-Definition-Video-Streaming and augmented reality applications [3], [4]. It is expected that this huge data exchange will continue to increase in the next few decades leading representatives of industry and academia to look into the technological developments towards the next generation of mobile communications (5G) [4].

There is widespread agreement that 5G systems will have to rely on technologies that can offer a substantial increase in transmission capacity [5], through a combination of innovative techniques involving different network layers, without significant increase in bandwidth, and energy consumption [4].

In the physical layer, OFDM transmission system is currently a solution widely used in the 4G-LTE (Long Term Evolution) system, mainly due to its robustness against multipath channels and their relative simplicity of implementation based on the Fast Fourier transform (FFT) algorithm [1]. However, the OFDM transmission has some disadvantages such as limited spectral efficiency as a result of the need for a Cyclic Prefix band-guard (CP), intrinsic elevated side lobes that increase the Out-of-Band emission level (OOB), as well as the need for a high level of synchronization in order to maintain the orthogonality between OFDM subcarriers [5]. These factors are especially sensitives in some application scenarios predicted for the 5G such for instance the low power consumption demands in M2M communications turns unaffordable the strict synchronization required to keep the orthogonality between the OFDM subcarriers. In others applications such as Tactile Internet and vehicular communications (V2V) which require short bursts of data, the OFDM systems with one CP per symbol have low spectral efficiency.

Therefore, some alternative non-orthogonal multi-carrier waveforms possessing larger spectral efficiency and lower synchronizations requirements are being considered for 5G system [5], [6].

Among these waveforms, one that is receiving increasing attention in the literature is the GFDM. One of the main advantages of GFDM is its larger spectral efficiency comparing to that of the CP-OFDM because it uses only one CP per transmitted group of symbols instead of a CP per transmitted symbol as in the CP-OFDM. In the GFDM different filter impulse responses can be used to filter the subcarriers and thus reducing level of the OOB emissions. In addition, GFDM has robustness for synchronization errors [1].

In spite of aforementioned advantages, the GFDM system exhibits intrinsic interference between its subcarriers unlike CP-OFDM systems which has orthogonal subcarriers. For this reason, the development of interference cancellation techniques is critical. Specifically, the non-orthogonality between the waveforms used in GFDM makes imperative the development of detection algorithms with jointly suppression of inter carrier interference (ICI).

Detection schemes that employ Serial Interference Cancellation (SIC) strategies were proposed in [7], [8] in order to eliminate ICI in GFDM transmission systems. In these works a Zero Forcing (ZF) channel equalization is employed previously to the detection scheme, which requires the inversion of the channel matrix. This increases the complexity of the receiver especially for large receiving block of symbols.

The proposed detection scheme of this work employs Matched Filter (MF) equalization, which does not require the inversion of the channel matrix, in conjunction with the PIC technique. In addition, to reduce the number of operations required for detection, a strategy is developed to dynamically set the number of PIC iterations in each detection.

The remaining sections of this document are organized as follows: Section II, introduces a matrix model representing the signal vectors transmitted in the GFDM system. As in the case of OFDM systems, the model is adequate and convenient for examining possible detection techniques. Section III, presents the proposed detection scheme to be used in GFDM systems. Numerical results obtained from computer simulations, including comparisons with the OFDM systems are presented in Section IV. Section V, gives some conclusions.

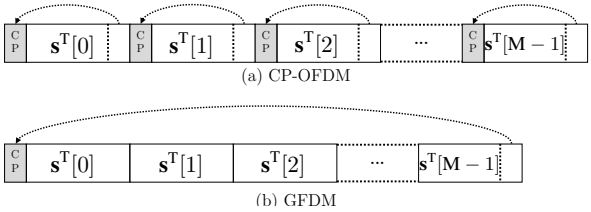

Fig. 1. (a), configuration of a data set in a CP-OFDM system. (b), configuration of a data set in a GFDM system.

II. GFDM System Discrete Model

The main difference between the GFDM and CP-OFDM transmission techniques is that in the GFDM system the CP precedes a block of MN information symbols, transmitted using M time-slots and N subcarriers, while the CP-OFDM system uses one CP per block of N information symbols, transmitted by N subcarriers. As a consequence the throughput in the GFDM system is higher than that in the CP-OFDM system, thus implying higher spectral efficiency. However, since the GFDM subcarriers are not orthogonal then, unlike CP-OFDM, ICI-type interference arises. Hence, the proper choice of the GFDM formating pulse shape is critical to limiting the ICI phenomenon and the OOB emissions.

A schematic illustration of the data sets for the two systems is shown in Figure 1.

Following the development in [9], in order to generate the GFDM signal vector, we first consider the vectors $\mathbf{x}[m],\ m = 0, 1, 2, \cdots, M$, of dimension MN as indicated in (1). The signal vector to be transmitted, $\mathbf{x}$, is obtained by adding circularly shifted versions of $\mathbf{x}[m]$, with period mN, as indicated in (2).

$$\mathbf{x}[m] = \mathbf{p} \odot \left(\mathbf{W}_{\mathrm{MN}}^{\mathrm{H}} \mathbf{s}_{\mathrm{e}}[m]\right) \quad , \quad \mathbf{p} = \mathbf{W}_{\mathrm{MN}}^{\mathrm{H}} \mathbf{c}_1 \quad , \tag{1}$$

$$\mathbf{x} = \sum_{m=0}^{M-1} \mathrm{circshift}\left(\mathbf{x}[m], m\mathrm{N}\right) \quad , \tag{2}$$

where the symbol $\odot$ denotes point-wise product, $\mathbf{W}_{\mathrm{MN}}^{\mathrm{H}}$, represents MN point iDFT and $\mathbf{s}_{\mathrm{e}}[m]$ $(m = 0, 1, \cdots, \mathrm{M}-1)$, is an expanded version of the vector $\mathbf{s}[m] = \left[s_0[m]\ s_1[m] \cdots\ s_{\mathrm{N}-1}[m]\right]^{\mathrm{T}}$, given by:

$$\mathbf{s}_{\mathrm{e}}[m] = \left[s_0[m]\ \mathbf{Z}_{\mathrm{M}-1}\ s_1[m]\ \mathbf{Z}_{\mathrm{M}-1} \cdots s_{\mathrm{N}-1}[m]\ \mathbf{Z}_{\mathrm{M}-1}\right]^{\mathrm{T}}, \tag{3}$$

with $\mathbf{Z}_{\mathrm{M}-1}$, denoting a vector of zeros of size $(\mathrm{M}-1)$. Also in (4) the discrete formating pulse $\mathbf{p} = \mathbf{W}_{\mathrm{MN}}^{\mathrm{H}} \mathbf{c}_1$, where

$$\mathbf{c}_1 = \left[c_0\ c_1\ \cdots\ c_{\mathrm{C}-1}\ 0\ \cdots\ 0\ c_{\mathrm{C}-1}\ c_{\mathrm{C}-2}\ \cdots\ c_1\right]^{\mathrm{T}} \tag{4}$$

corresponds to the discrete spectrum of the discrete pulse $\mathbf{p}$. The choice of coefficients $c_k,\ k \in [0, \mathrm{C}-1]$, is part of the design of the formating pulse on which the performance of the system depends heavily. Here we have used the set of coefficients suggested in [10] and [11]. It is important to note that the computational complexity of (1) is determined by the iDFT of the vector $\mathbf{s}_{\mathrm{e}}[m]$. However, taking into account the expanded structure of $\mathbf{s}_{\mathrm{e}}[m]$, it can be verified that the product $\mathbf{W}_{\mathrm{MN}}^{\mathrm{H}} \mathbf{s}_{\mathrm{e}}[m]$, can be obtained by stacking M repetitions of the product $\mathbf{W}_{\mathrm{N}}^{\mathrm{H}} \mathbf{s}[\mathrm{m}]$. That is, the generation of $\mathbf{x}[m]$ in (1), requires only a N point iDFT and one point-wise vector product, as follows [9]

$$\mathbf{x}[m] = \mathbf{p} \odot \begin{bmatrix} \mathbf{W}_{\mathrm{N}}^{\mathrm{H}} \mathbf{s}[m] \\ \mathbf{W}_{\mathrm{N}}^{\mathrm{H}} \mathbf{s}[m] \\ \vdots \\ \mathbf{W}_{\mathrm{N}}^{\mathrm{H}} \mathbf{s}[m] \end{bmatrix} \quad . \tag{5}$$

Although the vector $\mathbf{x}$ can be efficiently generated according to (2) and (5), it is convenient to express the vector $\mathbf{x}$ in a way similar to the known model used in the CP-OFDM signal representation. This matrix model is useful for the definition and analysis of possible detection methods for the GFDM system. To this, we define $\mathbf{D} = \mathrm{Diag}(\mathbf{p})$, where $\mathrm{Diag}(\mathbf{p})$ is the diagonal matrix that contains in its main diagonal the vector $\mathbf{p}$, and express the vector $\mathbf{x}[m]$ in (5) as follows

$$\mathbf{x}[m] = \mathbf{D} \begin{bmatrix} \mathbf{I}_{\mathrm{N}} \\ \mathbf{I}_{\mathrm{N}} \\ \vdots \\ \mathbf{I}_{\mathrm{N}} \end{bmatrix} \mathbf{W}_{\mathrm{N}}^{\mathrm{H}} \mathbf{s}[m] = \mathbf{Y}\mathbf{s}[m] \quad , \tag{6}$$

where $\mathbf{I}_{\mathrm{N}}$, represents a size N identity matrix and the matrix $\mathbf{Y}$ is defined by

$$\mathbf{Y} = \mathbf{D}\mathbf{I}\mathbf{W}_{\mathrm{N}}^{\mathrm{H}} \quad , \tag{7}$$

with $\mathbf{I} = \left[\mathbf{I}_{\mathrm{N}}\ \ \mathbf{I}_{\mathrm{N}}\ \ \cdots\ \ \mathbf{I}_{\mathrm{N}}\right]^{\mathrm{T}}$. Thus an alternative way to represent the vector $\mathbf{x}$ in (2), is given by

$$\mathbf{x} = \sum_{m=0}^{M-1} \mathbf{C}_{m\mathrm{N}} \mathbf{x}[m] = \sum_{m=0}^{M-1} \mathbf{C}_{m\mathrm{N}} \mathbf{Y}\mathbf{s}[m] \quad , \tag{8}$$

where the matrix $\mathbf{C}_{m\mathrm{N}}$ is such that its multiplication by a size MN vector is equivalent to performing mN circular shifts on that vector $(\mathbf{C}_{m\mathrm{N}} = \mathbf{C}_{\mathrm{N}}^{m})$. Then, by rewriting (8) in matrix form and taking (6) into account, we arrive at

$$\mathbf{x} = \underbrace{\left[\mathbf{Y}\ \ \mathbf{C}_{\mathrm{N}}\mathbf{Y}\ \ \mathbf{C}_{\mathrm{N}}^{2}\mathbf{Y}\ \ \cdots\ \ \mathbf{C}_{\mathrm{N}}^{(\mathrm{M}-1)}\mathbf{Y}\right]}_{\mathbf{B}} \underbrace{\begin{bmatrix} \mathbf{s}[0] \\ \mathbf{s}[1] \\ \vdots \\ \mathbf{s}[\mathrm{M}-1] \end{bmatrix}}_{\mathbf{s}_{\mathrm{a}}} . \tag{9}$$

Thus, the signal vector $\mathbf{x}$ in the GFDM system can be represented as a multiplication of a (MN×MN) matrix by the size MN vector of information symbols, as

$$\mathbf{x} = \mathbf{B}\mathbf{s}_{\mathrm{a}} \quad , \tag{10}$$

where $\mathbf{s}_{\mathrm{a}}$, is the vector that stacks the M vectors of N symbols organized in the GFDM information package as shown in the example of Figure 1 (b). Figure 2 illustrates the components of the matrix $\mathbf{B}$ for a particular choice of parameters.

III. Joint Detection and Subcarrier Interference Cancellation in the GFDM Transmission System

In this section the MF detection method for GFDM systems is presented. In addition, a preliminary analysis of the parallel interference cancellation method, PIC, is performed.

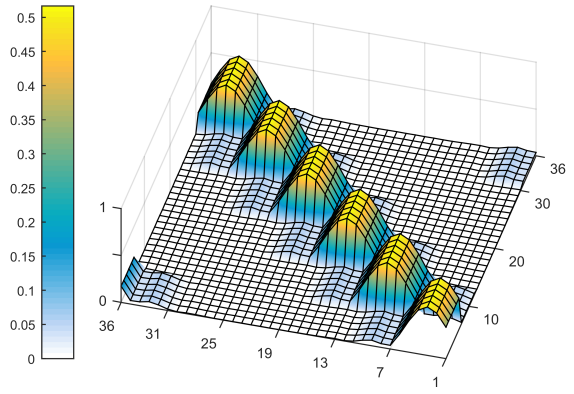

Fig. 2. Elements of the **B** Matrix for the parameters: M = 6 symbols, N = 6 subcarriers. The coefficients used in 4 are the ones in Table I.

A. MF Detection in the GFDM System

A model for the transmitted signal is conveniently expressed in matrix form by (10) as $\mathbf{x} = \mathbf{B}\mathbf{s}_\mathrm{a}$. Thus, the transmission/reception process occurs as follows: after addition of the CP, with a length of G samples, the complex components of the resulting vector of dimension $\mathrm{MN}+\mathrm{G}$, where $\mathrm{G} \leq \mathrm{MN}$, are sent at a rate $\mathrm{R_s}$, using a phase and quadrature type of transmission and a transmission pulse $g_t(t)$, through a multipath channel. At reception, after demodulation, filtering by a detection filter matched to $g_t(t)$, and sampling at the symbol rate R_s, a vector containing the $\mathrm{MN}+\mathrm{G}$ samples is obtained. After CP removal the received vector can be expressed in the matrix form as

$$\mathbf{r} = \mathbf{A}\mathbf{s}_\mathrm{a} + \mathbf{n} \quad , \quad \mathbf{A} = \mathbf{H}\mathbf{B} \ , \tag{11}$$

where $\mathbf{r}$ is the received signal vector of dimension MN, $\mathbf{H}$ is a circulant (MN×MN) matrix related to the multipath channel[1]. The components of the symbol vector $\mathbf{s}_\mathrm{a}$ have variance $\sigma_\mathrm{s}^2 = \mathrm{E}[|s_i|^2] = E_\mathrm{s}$ and $\mathbf{n}$ is the vector that contains the samples of the noise present in the receiver after filtering by detection filter with covariance matrix given by $\mathbf{K_n} = \mathrm{E}[\mathbf{n}\mathbf{n}^\mathrm{H}] = \mathrm{N}_0\mathbf{I}$, being $\frac{\mathrm{N}_0}{2}$ the power spectral density level of the AWGN noise at the input of the receiver.

An MF operation is then applied to the received vector $\mathbf{r}$, resulting in the signal

$$\mathbf{r}_\mathrm{MF} = \mathbf{A}^\mathrm{H}\mathbf{r} = \mathbf{A}^\mathrm{H}\mathbf{A}\mathbf{s}_\mathrm{a} + \mathbf{n}_\mathrm{MF} \quad , \tag{12}$$

where $\mathbf{n}_\mathrm{MF} = \mathbf{A}^\mathrm{H}\mathbf{n}$ and $\mathbf{A}^\mathrm{H} = \mathbf{B}^\mathrm{H}\mathbf{H}^\mathrm{H}$. An estimate of the symbol vector can be obtained from (12), by means of

$$\hat{\mathbf{s}}_\mathrm{a} = Q(\mathbf{r}_\mathrm{MF}) \quad , \tag{13}$$

where the function $Q(\cdot)$ maps each component of the vector $\mathbf{r}_\mathrm{MF}$ into the nearest symbol belonging to the signal constellation of the modulation employed in the system.

[1]The first column of H contains the zero-padded discrete equivalent low-pass impulse response of the multipath channel. It is assumed that the length L of this impulse response does not exceed the length G of the CP ($\mathrm{L}-1 \leq \mathrm{G} \leq \mathrm{MN}$).

TABLE I
SET OF COEFFICIENTS USED IN THE GENERATION OF **p**

c_0	c_1	c_2	c_3	c_4	c_5	c_6
1,000000	-0,999381	0,978386	-0,843901	0,536499	-0,206789	0,035185

B. MF-PIC Detector with Stop Strategy Based on the ML Metric

In this section the MF-PIC method is presented. This interference cancellation method is alternative to methods already considered for the GFDM system in which the formatting pulses Raised Cosine (RC) and Root Raised Cosine (RRC) are used [7], [12]. The related matrices obtained in those cases have higher concentration of energy outside the main diagonal, thus, resulting in a higher level of interference. The proposed MF-PIC for simultaneous detection and cancellation of interference in the GFDM system proposed here proves to be adequate because it is flexible and adaptable to various GFDM data packet configurations (different values of M and N).

The MF-PIC method generates successive estimates of $\mathbf{s}_\mathrm{a}$ by means of

$$\hat{\mathbf{s}}_\mathrm{a}^{(k)} = Q\left(\mathbf{z}^{(k)}\right) \quad , \tag{14}$$

where

$$\mathbf{z}^{(k)} = \mathbf{A}^\mathrm{H}\mathbf{r} - \left(\mathbf{A}^\mathrm{H}\mathbf{A}\right)_0 \hat{\mathbf{s}}_\mathrm{a}^{(k-1)} \quad , \quad k = 1, 2, \ldots \tag{15}$$

and $\left(\mathbf{A}^\mathrm{H}\mathbf{A}\right)_0$, corresponds to the matrix $\mathbf{A}^\mathrm{H}\mathbf{A}$, with zeros in its main diagonal.

By means of the recursion in (14) and (15), estimates of the symbols are generated sequentially up to a maximum number, K, of iterations. It should be emphasized here that due to the possible propagation of errors it is not guaranteed that the quality of the estimates improves with the number of iterations. Taking this fact into consideration, in the procedure proposed here the process can be interrupted in the k-th iteration ($1 \leq k \leq \mathrm{K}$) depending on the quality of the estimate generated. Here, this quality was measured by the Maximum Likelihood (ML) metric, which in the present case corresponds to the Minimum Distance (MD) metric, where the distance measure given by:

$$\mathrm{D}(\mathbf{x}) = \|\mathbf{r} - \mathbf{A}\mathbf{x}\|^2 \quad , \tag{16}$$

Thus, whenever there is a reduction in the quality of a given estimate, that is, $\mathrm{D}\left(\hat{\mathbf{s}}_\mathrm{a}^{(k)}\right) > \mathrm{D}\left(\hat{\mathbf{s}}_\mathrm{a}^{(k-1)}\right)$, the estimate $\hat{\mathbf{s}}_\mathrm{a}^{(k-1)}$ is adopted as the final estimate. The detection procedure is summarized in the pseudo-code illustrated in Figure (3).

IV. SIMULATION RESULTS

The following curves illustrate the performance of the proposed GFDM system when BPSK modulation is adopted and recursive MF-PIC is applied, the performance results are compared to those obtained with a CP-OFDM system using the usual ZF equalization in the frequency domain. The coefficients suggested in [11] for the construction of the formating pulse **p** are shown in Table I.

Data: First estimate of the GFDM symbols $\left(\hat{\mathbf{s}}_{\mathrm{a}}^{(0)}\right)$
Result: Final estimate of the GFDM symbols $(\hat{\mathbf{s}}_{\mathrm{af}})$
START
do $\mathrm{D}\left(\hat{\mathbf{s}}^{(0)}\right)$ % Performs the MD_0 metric
do Saves MD_0
for $k = 1, 2, \ldots, \mathrm{K}$ **do**
  Performs the PIC, (15)
  $Q(\cdot)$ Estimate the symbols, (14)
  Save the estimate $\hat{\mathbf{s}}_{\mathrm{a}}^{(k)}$
  $\mathrm{D}\left(\hat{\mathbf{s}}_{\mathrm{a}}^{(k)}\right)$ % Performs the MD_k metric
  % Compare the saved metric with the present metric
  if $\mathrm{MD}_k > \mathrm{MD}_{k-1}$ **then**
    Stops the process and provides the estimate $\hat{\mathbf{s}}_{\mathrm{af}} = \hat{\mathbf{s}}_{\mathrm{a}}^{(k-1)}$
  end
end
Provides the estimate $\hat{\mathbf{s}}_{\mathrm{af}} = \hat{\mathbf{s}}_{\mathrm{a}}^{(\mathrm{K})}$
END

Fig. 3. Algorithm for signal detection in the GFDM system using the MF-PIC technique and the ML metric.

TABLE II
CHANNEL MODELS

Channel	Discrete impulse response	Delay
AWGN	$h_0 = 1$	0
Multipath Channel	$h_{0_i} = 10^{\left(\frac{-i}{\mathrm{L}-1}\right)}{}_{i=1,2,\cdots,\mathrm{L}-1}$	$\mathrm{L}-1$

In the simulations the impulse response of the multipath channel is normalized to unitary energy ($\|\mathbf{h}\|^2 = 1$), $\mathbf{h} = \frac{\mathbf{h}_0}{\|\mathbf{h}_0\|}$, and the length of the CP guard band is given by $\mathrm{G} = \mathrm{L}-1$. The multipath channel model used and the simulation parameters are summarized in the tables II and III.

Figure 4, illustrates the information symbol error rate (SER) performance of the considered systems when operating in the AWGN channel. It can be observed that the GFDM MF-PIC performance is very close to that of the CP-OFDM system. We recall that both systems use 8-point iDFTs, and therefore they have a similar complexity concerning signal generation.

In the multipath channel case with $\mathrm{L} = 2$ coefficients, Figure 5, the MF-PIC detector required at most 4 iterations, with 1,75 as the average number of iterations, in order to reach the performance of the CP-OFDM system.

The results in Figure 6, indicate that with the MF-PIC detector the GFDM system outperforms the CP-OFDM when the two systems operate in a channel with $\mathrm{L} = 8$ multipath coefficients. The significant advantage of the GFDM system in terms of spectral efficiency is also evidenced. For the

TABLE III
SIMULATED SYSTEM CHARACTERISTICS

	OFDM	GFDM
Modulation	BPSK	BPSK
Time-slots (M)	1	8
Subcarriers (N)	8	8
Formatting Pulse Coefficients (C)	-	7 (Table I)
Channel (L)	AWGN, 2, 8	AWGN, 2, 8
Number of bits transmitted	$19,2 \times 10^6$	$19,2 \times 10^6$

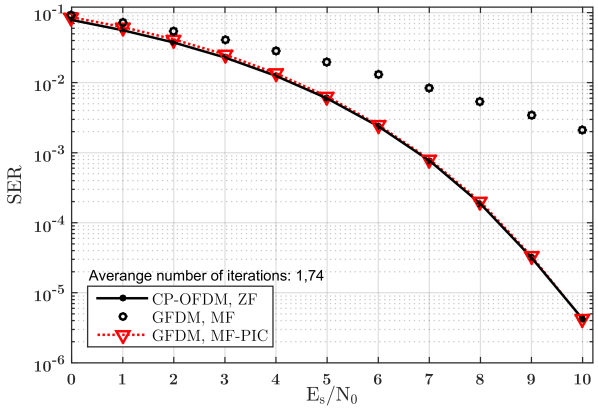

Fig. 4. SER performance of the GFDM MF-PIC detector in the AWGN channel ($\mathbf{A} = \mathbf{B}$). $\mathrm{M_G} = \mathrm{N_G} = 8$, $\mathrm{C} = 7$, $\mathrm{K} = 10$. Transmission of 8-symbol vectors for the CP-OFDM system. Transmission of $19,2 \times 10^6$ information symbols.

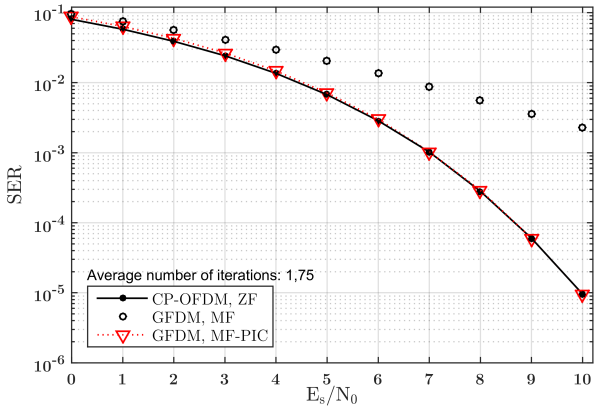

Fig. 5. SER performance of the GFDM MF-PIC detector in the $L = 2$ multipath channel ($\mathbf{A} = \mathbf{HB}$). $\mathrm{M_G} = \mathrm{N_G} = 8$, $\mathrm{C} = 7$, $\mathrm{K} = 10$. Transmission of 8-symbol vectors for the CP-OFDM system. Transmission of $19,2 \times 10^6$ information symbols.

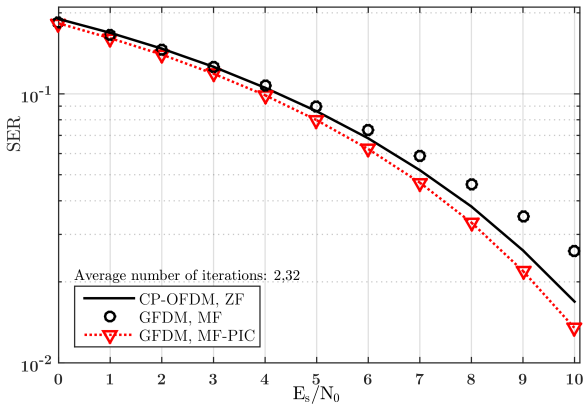

Fig. 6. SER performance of the GFDM MF-PIC detector in the $L = 8$ multipath channel ($\mathbf{A} = \mathbf{HB}$). $\mathrm{M_G} = \mathrm{N_G} = 8$, $\mathrm{C} = 7$, $\mathrm{K} = 10$. Transmission of 8-symbol vectors for the CP-OFDM system. Transmission of $19,2 \times 10^6$ information symbols.

TABLE IV
COMPARISON OF COMPLEXITY FOR DIFFERENT GFDM TRANSMITTERS

Technique	**Number of Complex Multiplications**	**Results M = N = 8**	**Results M = N = 64**
Direct **B** array multiplication	$(\mathrm{MN})^2$	4096	16777216
GFDM transmitter proposed in [13]*	$\mathrm{MN}(\log_2\mathrm{N} + 2\log_2\mathrm{M} + \mathrm{X})$	704	81929
GFDM transmitter proposed in [14]	$\frac{\mathrm{MN}}{2}(\log_2\mathrm{N} + \mathrm{M})$	352	143360
GFDM transmitter used in this work	$\frac{\mathrm{MN}}{2}(\log_2\mathrm{N} + 4)$	224	20480

* A typical value for parameter X is 2, [13].

channel with $\mathrm{L} = 8$ coefficients and $\mathrm{G} = 7$, for example, the spectral efficiency of the CP-OFDM system is $\eta_{OFDM} = \frac{N}{N+G} = \frac{8}{8+7} \cong 0,533$(bits/s/Hz), and for the GFDM system we have $\eta_{GFDM} = \frac{MN}{MN+G} = \frac{64}{64+7} \cong 0,901$(bits/s/Hz), thus achieving a spectral efficiency 1,7 times higher than the CP-OFDM system.

A direct comparison of the computational complexity of the GFDM transmitter used in this work with implementations of the transmitter presented in previous works is illustrated in Table IV.

V. CONCLUSIONS

In this work, we have presented and discussed a detection technique employing matched filtering and parallel interference cancellation to be used in GFDM systems. The matrix model for the GFDM transmitted signals, presented in Section II, allowed the analysis of MF detector performance. Moreover, we have analyzed the performance of the proposed method of interference cancellation, which is needed to minimize the ICI and ISI interference originated by the non-orthogonality of the GFDM subcarriers.

Besides offering a substantially higher gain in terms of spectral efficiency, especially for large channel delays, we have verified that the proposed method of detection MF-PIC for the GFDM systems has a performance, in terms of SER, almost identical to that of the CP-OFDM in environments with low channel delays and even superior with higher channel delays. It is worth noting that, unlike previously suggested implementations, the proposed method of detection does not require channel matrix inversions therefore reducing its implementation complexity.

REFERENCES

[1] Michailow N., Matthé M., Gaspar I.S., Caldevilla A.N., Mendes L.L., Festag A., & Fettweis G., *Generalized Frequency Division Multiplexing for 5th Generation Cellular Networks*, in IEEE Transactions on Communications, vol. 62, no. 9, (2014), pp. 3045–3061, ISSN 0090-6778, doi:10.1109/TCOMM.2014.2345566, September 2014.

[2] Farhang A., Marchetti N., Figueiredo F., & Miranda J.P., *Massive MIMO and Waveform Design for 5th Generation Wireless Communication Systems*, pp. 70–75, doi:10.4108/icst.5gu.2014.258195, November 2014.

[3] Chen S. & Zhao J., *The Requirements, Challenges, and Technologies for 5G of Terrestrial Mobile Telecommunication*, in IEEE Communications Magazine, vol. 52, no. 5, (2014), pp. 36–43, ISSN 0163-6804, doi: 10.1109/MCOM.2014.6815891, May 2014.

[4] Akyildiz I.F., Melodia T., & Chowdury K.R., *Wireless Multimedia Sensor Networks: A survey*, in IEEE Wireless Communications, vol. 14, no. 6, (2007), pp. 32–39, ISSN 1536-1284, doi: 10.1109/MWC.2007.4407225, December 2007.

[5] Banelli P., Buzzi S., Colavolpe G., Modenini A., Rusek F., & Ugolini A., *Modulation Formats and Waveforms for 5G Networks: Who will be the heir of OFDM?: An overview of alternative modulation schemes for improved spectral efficiency*, in IEEE Signal Processing Magazine, vol. 31, no. 6, (2014), pp. 80–93, ISSN 1053-5888, doi: 10.1109/MSP.2014.2337391, November 2014.

[6] Wunder G., Jung P., Kasparick M., Wild T., Schaich F., Chen Y., Brink S.T., Gaspar I., Michailow N., Festag A., Mendes L., Cassiau N., Ktenas D., Dryjanski M., Pietrzyk S., Eged B., Vago P., & Wiedmann F., *5GNOW: Non-Orthogonal, Asynchronous Waveforms for Future Mobile Applications*, in IEEE Communications Magazine, vol. 52, no. 2, (2014), pp. 97–105, ISSN 0163-6804, doi: 10.1109/MCOM.2014.6736749, February 2014.

[7] Alves B.M., Mendes L.L., Guimaraes D.A., & Gaspar I.S., *Performance of GFDM Over Frequency-Selective Channels – Invited Paper*, November 2013.

[8] Gaspar I., Michailow N., Navarro A., Ohlmer E., Krone S., & Fettweis G., *Low Complexity GFDM Receiver Based on Sparse Frequency Domain Processing*, pp. 1–6, ISSN 1550-2252, doi: 10.1109/VTCSpring.2013.6692619, June 2013.

[9] Farhang-Boroujeny B. & Moradi H., *Derivation of GFDM Based on OFDM Principles*, pp. 2680–2685, ISSN 1550-3607, doi: 10.1109/ICC.2015.7248730, June 2015.

[10] Martin K.W., *Small Side-Lobe Filter Design for Multitone Data-Communication Applications*, in IEEE Transactions on Circuits and Systems II: Analog and Digital Signal Processing, vol. 45, no. 8, (1998), pp. 1155–1161, ISSN 1057-7130, doi:10.1109/82.718830, August 1998.

[11] Mirabbasi S. & Martin K., *Overlapped Complex-Modulated Transmultiplexer Filters with Simplified Design and Superior Stopbands*, in IEEE Transactions on Circuits and Systems II: Analog and Digital Signal Processing, vol. 50, no. 8, (2003), pp. 456–469, ISSN 1057-7130, doi: 10.1109/TCSII.2003.813592, August 2003.

[12] Michailow N., Lentmaier M., Rost P., & Fettweis G., *Integration of a GFDM Secondary System in an OFDM Primary System*, pp. 1–8, June 2011.

[13] Michailow N., Gaspar I., Krone S., Lentmaier M., & Fettweis G., *Generalized Frequency Division Multiplexing: Analysis of an Alternative Multi-Carrier Technique for next Generation Cellular Systems*, pp. 171–175, ISSN 2154-0217, doi:10.1109/ISWCS.2012.6328352, August 2012.

[14] Farhang A., Marchetti N., & Doyle L., *Low Complexity Transceiver Design for GFDM*, January 2015.